RSC Advances

ROYAL SOCIETY OF CHEMISTRY

www.rsc.org/advances

Journal Name

ARTICLE

Activity-tunable nanocomposites based on dissolution and *in situ* recrystallization of nanoparticles on ion exchange resins

Amanda Alonso[a,*], Núria Vigués[b], Rosalía Rodríguez-Rodríguez[c], Xavier Borrisé[d], María Muñoz[e], Dmitri N. Muraviev[e], Jordi Mas[b] and Xavier Muñoz-Berbel[f,*]

This work proposes the use of cationic Ion Exchange Resins as a platform for *in situ* formation and recrystallization of nanoparticles as a way to dynamically modulate their activity by changing their structure/ composition. Here applied to Ag@Co-nanoparticles in cationic resins, this protocol may be expanded to other materials, opening the possibility to modulate activity with a simple and economic approach.

Introduction

Polymer nanotechnology provides with simple and quick synthetic routes for the development of low-cost functional materials with improved functionalities [1]. One of the most interesting routes is InterMatrix Synthesis (IMS), where ionic precursors of the metal are loaded in a polymer and reduced *in situ* to obtain metal nanoparticles (NPs) [2]. With this protocol, single-metal and bimetallic core-shell NPs have been already synthesized in polymeric matrices of different nature (e.g. membranes [3], fibers [4] or resins [5]).

The role of the polymeric matrix in IMS is twofold. First, it acts as supporting material, retaining the ionic precursors for subsequent NPs formation. Additionally, it also acts as stabilizing agent, ensuring homogeneous distribution of the NPs thus avoiding their aggregation and leakage. Conversely, NPs are the functional element in the structure, conferring the nanocomposite with the desired activity. This may be catalytic capacity [6, 7], antibacterial activity [2, 8] and/or magnetism [9]. As a step forward, the activity of nanocomposites containing bimetallic NPs is the combination of the activity of both NPs [10]. In some cases, synergetic effects, due to the combination of two metals in a single core-shell NP

(shell@core), have been reported. For instance, in the Ag@Co-nanocomposite reported by our group, the presence of Co in the core enhanced bactericidal activity of the Ag shell [4]. Hence, IMS provides with a very versatile synthetic route to obtain nanocomposites with different activities through a simple and fast synthetic protocol. Their main limitation may be in terms of versatility. Traditional IMS protocols are designed to produce nanocomposites with a selected activity, which remain stable over time. However, it is not possible to modulate or change their activity once fabricated.

Regarding this, and according to bibliography [11], NPs activity can be modulated by altering their size, shape, composition or state of aggregation. Hence, the activity of a nanocomposite may be tailored by modifying some of the previously exposed properties of the NPs.

Based on the latter, this communication proposes an IMS protocol to produce dynamic and activity-tunable nanocomposites based on the modification of Ag@Co-NPs stabilized on Ion Exchange Resins (IER).

Experiment

InterMatrix synthesis protocol for Ag@Co-NPs in sulfonated IER

The raw sulfonated polymeric resin was initially pre-treated with 0.1 M NaCl (1 h) to ensure the presence of Na^+ as counterion in the resin. In the synthesis of bimetallic Ag@Co NPs, Co-NPs were firstly synthesized by loading the pre-treated polymer with 0.01 M $Co(NO_3)_2$ (1 h) and reduction to Co^0 with 0.5 M $NaBH_4$. Next, the material containing Co-NPs was loaded with 0.01 M $AgNO_3$ solution for 30 min and the Ag^+ was reduced to Ag^0 by addition of 0.5 M $NaBH_4$. Core-shell bimetallic Ag@Co NPs were thus obtained in the polymeric material structure [12].

Incubation conditions of the pre-synthesized Ag@Co NPs for activity-tune evaluation

a. Chemical Engineering Departament. Escola d'Enginyeria. Universitat Autònoma de Barcelona, UAB, Spain
b. Department of Genetics and Microbiology, UAB, Spain
c. Department of Pharmacology, Universidad de Sevilla, Spain
d. Institut Català de Nanociencia i Nanotecnología (ICN2), Spain
e. Department of Chemistry, UAB, Spain
f. Centre Nacional de Microelectrònica (IMB-CNM, CSIC), Bellaterra, Spain
† Footnotes relating to the title and/or authors should appear here.
g. Electronic Supplementary Information (ESI) available: [SI.1. SEM images for the nanostructures obtained by modifying the incubation conditions, SI.2. EDX spectra corresponding to nanocomposites containing NPs, CSs or FLSs. The spectrum corresponding to the IER without modification is also added for comparison and SI.3. Histograms showing the size frequency of the nanostructures for different incubation conditions.
h.]. See DOI: 10.1039/x0xx00000x

Pre-synthesized Ag@Co-NPs on sulfonated IER were incubated in aqueous solutions containing different concentrations of chloride (from 0.5 to 1.0M) and/or phosphate (from 0.05 to 1.0M) at different temperatures (4, 37, 60, 80°C) for 16 h. After that, samples were dried and stored at 4°C until analysed. Control sample consisted of sulfonated polymer without pre-synthesized NPs.

Scanning Electron Microscope (SEM) Imaging and Energy Dispersive X-ray Spectroscopy (EDX) analysis

Experimental samples were analysed with a SEM (Merlin FE-SEM, Zeiss) coupled to an EDX from Servei de Microscopia of the UAB. EDX provided the metal chemical composition of the samples based on the X-Rays emitted by an atom which interacted with an electron beam. Each atom has a unique X-ray spectrum and so the elemental composition could be obtained by the detected radiation. EDX spectra were always obtained at 20keV for being the one calibrated and allowing semi-quantitative analysis. NPs, aggregates, FLS and CS morphology, distribution and composition were obtained. Additionally, information about size was obtained after SEM images analysis using the free-software ImageJ.

X-Ray Diffraction (XRD)

XRD technique was used to obtain the crystalline structure of the particles. In a diffraction pattern, the location of the peaks on the 2θ scale can be compared to reference peaks. Diffraction patterns were collected on Panalytical X´Pert PRO MPD (Multipurpose Diffractometer). Analyses were performed at Institut Català de Nanociència i Nanotecnologia (ICN2), Spain. The identification of magnetite was based on the characteristic peaks in the diffractograms and comparing with the database.

Bactericide Activity

Minimum Inhibitory Concentration (MIC) assay was performed to evaluate the bactericide activity of samples containing different aggregate architectures (i.e. NPs, FLS and/or CS). The MIC 50 is defined as the concentration of an antimicrobial agent that inhibits the proliferation of 50% of the microorganisms presents in a sample. In this case, the MIC 50 of each nanocomposite was determined by introducing an increasing amount of nanocomposite bead (the whole nanocomposite, without extraction of NPs) in individual wells of a 96-well ELISA plate already containing 200 μL of 10^5 colony forming units per mL (CFU/mL) of *Escherichia coli* (*E. coli*) in (Luria-Bertani) LB medium. After overnight incubation (16-18 h), bacterial proliferation was evaluated by measuring the optical density of each well at 550 nm using a SmartSpec Plus Spectophotometer (Biorad). The antibacterial activity of all nanocomposites was determined. The raw material without NPs was used as control.

Cytotoxicity Assay

Determination of cell viability is a common method to estimate biocompatibility of materials. The cytotoxicity of the samples containing different structures (i.e. NPs, FLS and/or CS) was evaluated in vascular smooth muscle cells (VSMC) cultured from rat aorta by using the colorimetric MTT (3-(4,5-dimethylthiazol-2-yl)-2,5-diphenyltetrazolium bromide) assay. This technique is based on the ability of viable cells to transform the MTT salt into formazan dyes. VSMCs were tripsinised and plated in a 96-well culture plate at 7·10^4 cell/well in Dulbecco's modified Eagle's medium (DMEM) (Gibco- Invitrogen, Spain). After 24 h attachment, a nanocomposite bead (the whole nanocomposite, without extraction of NPs) was introduced in the well an incubated with cells for another 24 h. Next, the nanocomposite was collected, the culture medium was aspirated and the wells were washed with PBS. The MTT solution (1 mg/mL) was added at each well and incubated for 4 h. The purple formazan generated by viable cells was solubilized with 20% sodium dodecyl sulphate in 0.02 M HCl and incubated for 10 h at 37 ^{o}C. Absorption of each well was determined at 540 nm in a Thermo Electron Multiskan EX plate reader (VWR International, Pennsylvania). Cell viability was expressed as percentage in relation to controls (non-treated cells).

Results and discussion

IER were used as a platform for *in situ* formation and recrystallization of NPs to architectures with modified structure, composition and function. To this end, core-shell Ag@Co-NPs in IER were incubated with solution and under experimental conditions that induced their dissolution and subsequent re-crystallization. The role of the polymeric matrix was fundamental at this stage. Negatively-charged sulfonated functional groups in the resin captured re-dissolved ionic precursors allowing the subsequent *in situ* recrystallization of NPs with minimal reagents losses.

Incubation solutions contained phosphate and chloride; two ions that interacted with Ag-NPs. Phosphate ions are capable to change the morphology of pre-synthetized Ag-NPs [13]. Chloride ions, on the other hand, can etch Ag-NPs, leading to the formation of regular aggregates [14]. Moreover, both chloride and phosphate react with Ag ions, being able to induce Ag re-crystallization to produce NPs of different composition (e.g. AgCl, AgCl@Co, Ag$_3$PO$_4$, etc.) and aggregation state. Apart from them, other components of the incubation solution may influence NPs dissolution and re-crystallization. This is the case of Co^{2+} ions. According to bibliography [4, 15], the presence of Co^{2+} traces, in this case from dissolved Ag@Co-NPs, may also induce Ag ions reduction and Ag-NPs formation. Thus, the equilibrium between both dissolution and recrystallization reactions may lead to the formation of NPs with different structure/function, allowing the dynamic modulation of nanocomposite activity.

In order to study the incubation-induced modulation of activity, nanocomposites were subjected to different incubation conditions. These included phosphate concentrations between 0 and 0.1 M, chloride concentrations from 0 to 0.67 M and temperatures from 4 to 80°C. SEM, EDX and XRD techniques were used to determine nanocomposite structure and composition at the different incubation situations (detail in Experimental Section).

COMMUNICATION

Equilibrium between dissolution and recrystallization reactions was reached under three experimental conditions ranges, detailed in Figure 1.

Figure 1 here

At these conditions, regular aggregate structures, i.e. fractal-like (FLS) and cubic structures (CS), were obtained. More precisely, FLS were observed in nanocomposites after incubation with phosphate solutions (0.05 or 0.1 M phosphate) at a temperature between 4 and 65°C. CS, on the other hand, were obtained after incubation with 0.5 M chloride at temperatures between 30 and 65°C. Both FLS and CS were observed in nanocomposite samples incubated with chloride (0.14 and 0.67 M) and phosphate (0.01 and 0.07 M) in a wide temperature window (4-80 °C). The number and size of FLS and CS in the sample depended on the incubation conditions. Representative images of nanostructures obtained under these experimental conditions and others used during activity modulation evaluation are available in Supplementary Information (SI.1). It should be mentioned that FLS in nanotechnology are commonly associated to processes involving formation of NPs. Concretely, it is reported that FLS are composed of multiple primary particles which act as nucleation centers in the synthesis of NPs [16].

The formation of these regular aggregates of NPs was associated to a dissolution-recrystallization process. XRD data from nanocomposite samples containing NPs, CS and FLSs is illustrated in Figure 2).

Figure2 here

As shown, all nanocomposites, independently on their composition/aggregation state, presented two phases. The first phase, the principal component of the spectrum was amorphous, and may be associated to the polymeric IER. The second one corresponded to the crystalline components, in this case, the NPs. Different crystalline peaks were observed depending on the nanostructures present in the nanocomposite. Unfortunately, only those corresponding to nanocomposites containing CS could be assigned to a crystalline structure. Concretely, these peaks presented strong similarity to AgCl crystals, which suggested that this may be the main component of the cubes. Spectra corresponding to nanocomposites containing NPs or FLSs could not be assigned to any single Ag and/or Co crystalline pattern, probably due to their low intensity or the presence of NPs with different composition. Even though, the differences in the crystalline phase corroborated NPs recrystallization during the incubation and their change of composition, depending on the incubation conditions.

In terms of composition, nanocomposite samples containing NPs, CSs and FLSs were analysed by EDX and compared with IER without nanostructures. EDX peaks comparison is illustrated in Figure 3 (EDX spectra in SI.2 Supplementary Information).

Figure 3 here

According to these results, CSs and FLSs presented Ag and Co concentrations higher than those recorded in other regions of the nanocomposite. Since no additional metal precursors were added during incubation, the formation of these structures with high Ag and Co concentration confirmed NPs dissolution and concentration before recrystallization. It was demonstrated by statistical analysis of aggregate size in the nanocomposite sample. Thus, nanocomposite samples containing CSs presented aggregates of NPs significantly bigger than those observed in nanocomposites without NPs. An example is illustrated in Figure SI.3. In this figure, the size of the aggregates observed after incubation with solutions containing 0, 0.5 and 1.0 M chloride at 30°C was determined and compared. According to results, 0.5 M chloride solutions, leading to CSs, presented bigger aggregates (163±26 μm average) than the others (140±34 μm for 0 M and 110±30 μm for 1.0 M chloride, respectively). Additionally, the concentration of chloride in cubes was higher than in other structures or other regions of the same nanocomposite. This result may confirm the presence of AgCl crystals in the nanocomposite structure.

The structural and composition changes observed (by SEM, EDX and XRD) may involve a modification of the nanocomposite activity. Bactericide and cytotoxic activity of Ag@Co-NPs synthesized *in situ* on IER has been already reported [12]. Following the same protocols, bactericide and cytotoxic activities of the modified nanocomposites reported here were determined and compared with previous results.

Nanocomposites containing either FLSs or CSs presented significantly lower bactericide activity than those containing NPs (MIC 50_{FLS} = 3.2±0.4 particle/200 μL; MIC 50_{CS} = 2.8±0.2 particle/200 μL; MIC 50_{NP} = 1.01±0.15 particle/200 μL; Figure 4).

Figure 4 here

This decrease may be the combination of factors. First, NPs aggregation to build big aggregates such as CSs or FLSs may drastically reduce the specific exposed bactericide surface. Apart

from that, activity reduction may be also attributed to composition changes. In this sense, AgCl is reported to be less bactericidal than Ag [17].

In terms of cytotoxicity, nanocomposites containing CSs were found much more cytotoxic (cell viability$_{NP}$ = 87±5 %; Figure 5) than those containing FLSs or NPs, which presented similar cytotoxicities (cell viability$_{FLS}$ = 113±1 %; cell viability$_{NP}$ = 114±2 %; Figure 5)

Figure 5 here

According to previous experiences, most of cytotoxicity associated to Most of cytotoxicity should be associated to Ag@Co-NPs may be attributed to Co [12]. In fact, Co is reported to be much more cytotoxic than Ag or any other component of the nanocomposite [19]. Then, this result suggested that the amount of Co in contact with cells was higher in samples with CS than in those only containing NPs or FLSs. This was partially corroborated by EDX analysis of nanocomposites containing CSs, where it was possible to find areas containing high concentrations of Co (Figure 6).

Figure 6 here

In this region, Ag may not be completely covering Co-NPs and hence, it may be in direct contact with cells, increasing samples cytotoxicity. Therefore, it may be possible to postulate that, apart from AgCl crystals (as we concluded above), nanocomposites containing CSs may also present Co-NPs with high cytotoxic activity. Thus, we observed here a modification of the bactericide activity, in comparison with the previous results reported for Ag@Co-NPs [12], when this material is treated under different incubation conditions.

Conclusion and References

IER can be used as a platform for *in situ* formation of NPs and their recrystallization to build NPs with modified structure/composition as a way to modulate their activity. This concept has been demonstrated with highly reactive Ag@Co-NPs synthesized on sulfonated IER by IMS. Structural-functional changes were achieved after overnight incubation with low concentrations of chloride and/or phosphate ions, which induced NPs dissolution and

recrystallization to regular aggregates (i.e. FLS and or CSs). FLSs and CSs presented low bactericidal activity because of NPs aggregation and their change in composition. Additionally, CSs showed and enhanced cytotoxic activity, probably due to the presence of Co-NPs. Hence, with a simple incubation step and under soft reaction conditions, it was possible to tune nanocomposites activity by modifying the aggregation state and composition of the NPs. This process, here demonstrated by highly reactive Ag@Co-NPs, may be applied to NPs with other composition by application of suitable reagents and experimental conditions.

‡ Footnotes relating to the main text should appear here. These might include comments relevant to but not central to the matter under discussion, limited experimental and spectral data, and crystallographic data.
§
§§
etc.

1   D.R. Paul, L.M. Robeson, Polymer, 2008, **49** (15), 3187
2   A. Alonso, N. Vigués, X. Muñoz-Berbel, J. Macanás, M. Muñoz, J. Mas, D.N. Muraviev. *Chem. Commun*., 2011, **47**, 10464
3   D.N. Muraviev, J. Macanás, J. Parrondo, M. Muñoz, A. Alonso, S. Alegret, M. Ortueta, F. Mijangos, *Reactive and Functional Polymers*, **67** (12), 2007, 1612
4   A. Alonso, N. Vigués, X. Muñoz-Berbel, J. Macanás, M. Muñoz, J. Mas, D.N. Muraviev. *Langmuir*, 2012, **28** (1), 783
5   A. Alonso, G.-L. Davies, A. Satti, J. Macanás, Y.K. Gun'ko, M. Muñoz and D.N. Muraviev, *Nanocomposites: In Situ Synthesis of Polymer-Embedded Nanostructures*, Wiley, 2012, ISBN 978-953-308-55-0
6   K. Esumi, R. Isono, and T. Yoshimura, *Langmuir*, 2004, **20** (1), 237
7   A. Alonso, D. N. Muraviev, J. Macanás, A. Shafir, M. Muñoz, A. Vallribera, D. Prodius, S. Melnic and C. Turta, *Dalton Trans*., 2010, **39**, 2579
8   R. Pinto, P. Marques, C. Neto, T. Trindade, S. Daina, P. Sadocco, *Acta Biomaterialia*, **5**, 2009, 2279
9   S. Behrens, *Nanoscale*, 2011, **3**, 877
10   F. Zhan and C. Zhang, *J. Mater. Chem.,* 2011, **21**, 4765
11   J. Jiang, G. Oberdorster, P. Biswas, *J. Nanopart. Res.*, 2009, **11**, 77
12   A. Alonso, X. Muñoz-Berbel, N. Vigués, R. Rodríguez-Rodríguez, J. Macanás, M. Muñoz, J. Mas and D. N. Muraviev. *Advanced Functional Materials*, 2013, **23** (19), 2450
13   J. Zhong-Jie, L. Chun-Yan, S. Lu-Wei, *J. Phys. Chem. B*. 2005, **109**, 1730
14   S. Chang, K. Chen, Q. Hua, Y. Ma, W. Huang, *J. Phys. Chem*. *C*. 2011, **115**, 7979.
15   A.R. Tao et al., Angew. Chem. 2006, **118**, 4713
16   M.L. Eggersdorfer, D. Kadau, H. J. Herrmann, S. E. Pratsinis, *Langmuir*, 2011, **27**, 6358
17   S. Agnihotri, S. Mukherjiabc and S. Mukherj, *Nanoscale*, 2013, **5**, 7328

Figure 1. Scanning Electron Microscope (SEM) image for samples incubated overnight in solutions containing 0.14 M chloride and 0.01 M phosphate at 30°C, here used to illustrate the architectures obtained after each incubation condition.
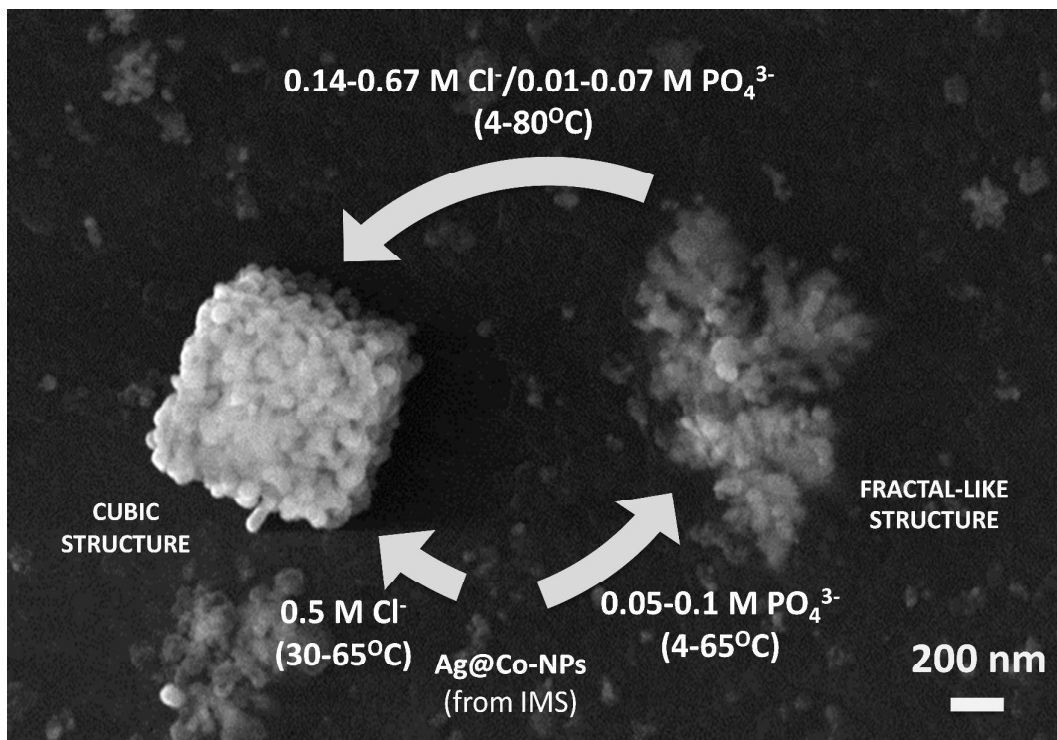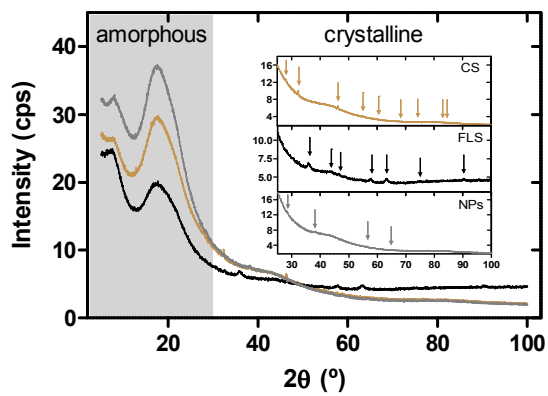
Figure 2. XRD analysis of nanocomposite samples containing NPs, FLS or CS. Inset, a magnification of the crystalline area of each samples indicating the crystalline peaks obtained with the analysis.
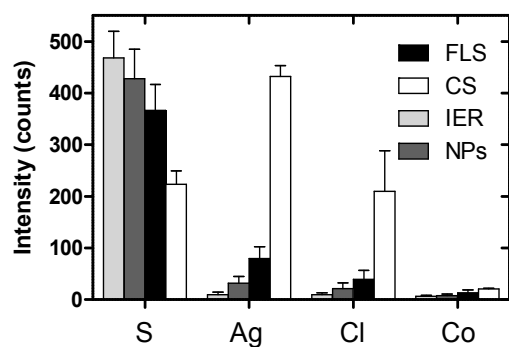
Figure 3. Pseudo-quantitative comparison of EDX peaks corresponding to Sulphur (S), Ag, chloride (Cl) and Co for nanocomposite samples containing NPs, FLS or CS. EDX measurements were performed at the calibrated energy of 20eV. IER without NPs modification was used as control for comparison reasons. Error bars correspond to the standard deviation of the measurement.
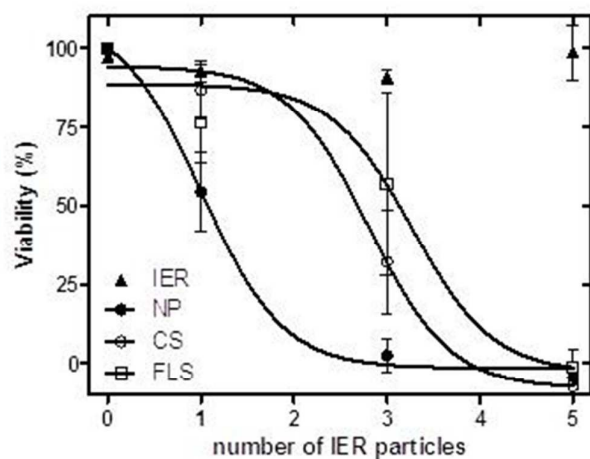
Sample	MIC 50 (particle/ 200µL)
IER	–
NP	1.01±0.15
CS	2.8±0.2
FLS	3.2±0.4

Figure 4. Bactericide activity. Representation of the variation of bacterial viability (in percentage terms) with the increasing number of nanocomposite for samples containing NPs, CSs or FLS. Error bars represent standard deviation from the mean (95 % confidence, n=3). The MIC 50 magnitude of each nanocomposite is included in the table inset.
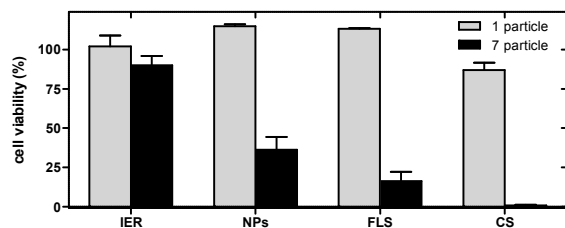
Figure 5. MTT cytotoxicity assay. Representation of cell viability of muscle cells after incubation with 1 or 7 particles of nanocomposite containing NPs, FLS or CS. IER alone was used as control. The percentage of cell viability was determined by comparison with samples without nanocomposite. Error bars represent standard deviation from the mean (95 % confidence, n=3).
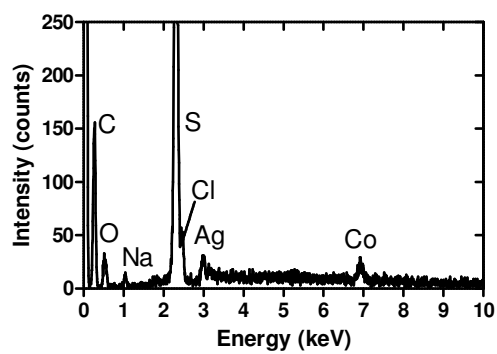
Figure 6. EDX spectrum of nanocomposites containing CSs where Co peak intensity is similar to that obtained by Ag.